第35卷第1期
2016年2月

红外与毫米波学报
J. Infrared Millim. Waves

Vol. 35, No. 1
February, 2016

文章编号: 1001 - 9014(2016)01 - 0021 - 04

DOI:10.11972/j.issn.1001 - 9014.2016.01.005

Smith-Purcell radiation in a grating-resonator composite structure

MENG Xian-Zhu*, WANG Ming-Hong, REN Zhong-Min

(Shandong Provincial Key Laboratory of Optical Communication Science and Technology,
School of Physics Science and Information Engineering, Liaocheng University, Liaocheng 252059, China)

Abstract: A grating-resonator composite structure was investigated. The output characteristics of Smith-Purcell radiation in this grating-resonator composite structure were studied by optical theoretic analysis and particle-in-cell simulation method. The results show that tunable coherent Smith-Purcell radiation at Terahertz wavelengths can be generated by this novel structure. This novel grating-resonator composite structure has the following advantages: it can reflect all radiation with an emission angle and random azimuthal angles which backs onto the electron beam with same phase and cause the electrons to be modulated.

Key words: electron physics, Smith-Purcell radiation, particle-in-cell simulation, grating-resonator composite structure

PACS: 07.57.-c, 41.60.Cr, 52.59.Rz, 42.60.Da

光栅—谐振腔复合结构中的史密斯—帕塞尔辐射

孟现柱*, 王明红, 任忠民

(聊城大学 物理科学与信息工程学院,山东省光通信科学与技术重点实验室, 山东 聊城 252059)

摘要:提出了光栅—谐振腔复合结构. 利用光学理论和粒子模拟方法研究了这种光栅—谐振腔复合结构中的史密斯—帕塞尔辐射的输出特性. 结果显示:利用这种装置可以产生太赫兹波段的可调谐相干史密斯—帕塞尔辐射. 这种光栅—谐振腔复合结构具有下列优点:它可以把一定发射角和任意方位角的史密斯—帕塞尔辐射同相位反馈到电子束,对电子束进行调制.

关 键 词:电子物理学;史密斯—帕塞尔辐射;粒子模拟;光栅—谐振腔复合结构

中图分类号:O436 **文献标识码**:A

Introduction

Electromagnetic radiation of moving charged particle (e.g. electron) passing over a periodic structure made of some metallic material, the so-called Smith-Purcell (S-P) effect[1-2], was predicted by Frank and observed by Smith and Purcell. In the S-P effect, the wavelength of the S-P radiation is determined by the S-P radiation formula

$$\lambda = \frac{l}{n}\left(\frac{1}{\beta} - \cos\theta\right) \quad , \quad (1)$$

where $\beta = v/c$ is the ratio of the electron's velocity to the velocity of light. l is the grating period, n is the order of the space harmonic wave, θ is the emission angle between the moving electron's direction and testing direction. Usually, the incoherent radiation from S-P effect is too weak to be used and detection of the signal is very difficult. To generate coherent radiation and amplify electromagnetic waves at millimeter and far-infrared wavebands, a feedback configuration is utilized in experiments[3-8]. In this letter, a novel feedback configuration is presented by our group. This feedback configuration is a grating-resonator composite structure. The output characteristics of this grating-resonator composite structure were studied by theoretic analysis and particle-in-cell (PIC) simulation method.

1 Basic Theoretical Background

The configuration of the experimental device of S-P radiation is schematically shown in Fig. 1. The grating-

Received date: 2015 - 01 - 12, **revised date**: 2015 - 06 - 23 **收稿日期**:2015 - 01 - 12, **修回日期**:2015 - 06 - 23

Foundation items: Supported by National Natural Science of China (11275089, 11375081)

Biography: MENG Xian-Zhu(1968-), Shandong Pingyi, Associate Professor, master. Research area involves Smith-Purcell free electron Laser. E-mail:

* **Corresponding author**: E-mail: mengxz@lcu.edu.cn

resonator composite structure is made up of elliptical resonator and grating, and the grating is etched on the inner surface of elliptical resonator. In this letter, this composite structure is called all-feedback resonator. Based on the all-feedback resonator, the experimental device of S-P radiation is composed of an electron gun, a collector and the all-feedback resonator.

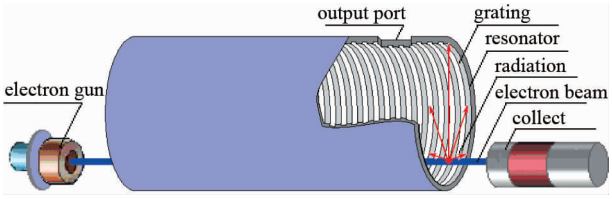

Fig. 1 Schematic diagram of the experimental device of S-P radiation. 图中英文有错:上方 colector 应改为 collect
图 1 S-P 辐射实验装置的示意图

The vertical plane of all-feedback resonator is shown in Fig. 2. According to the laws of reflection and the reflective characteristics of elliptical mirror, any ray from the focus, F_1, to the surface of elliptical mirror will be reflected back onto the other focus, F_2[9,10]. As shown in Fig. 2, the radiation ray in x-y plane e. g. F_1A, emitted by the electron beam at the focus, F_1, will be reflected back onto the focus, F_2, by the surface of elliptical mirror, e. g. AF_2B. For the same reason, the reflection ray, e. g. AF_2B, will be reflected back onto the focus, F_1, by the surface of elliptical mirror, e. g. BF_1C, and cause the electrons to be modulated. The reflection ray, e. g. BF_1C, will be reflected back onto the focus, F_2, by the surface of elliptical mirror, e. g. CF_2D, etc. The reflection ray, e. g. CF_2D, is reflected back onto the electron beam and toward the output port after multiple reflections.

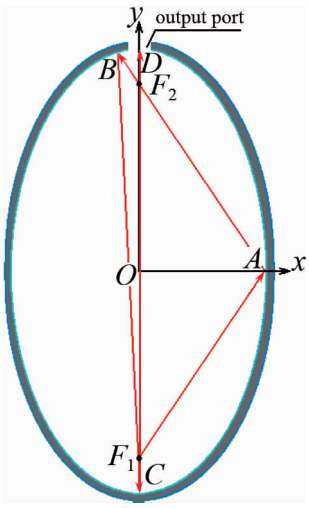

Fig. 2 Vertical plane of all-feedback resonator
图 2 全反馈谐振腔的剖面图

As shown in Fig. 2, the equations of elliptical mirror can be expressed as:

$$\frac{y^2}{a^2}+\frac{x^2}{b^2}=1 \quad , \quad (2)$$

where a is major half axis, and b is minor half axis. In the all-feedback resonator, when the radiation ray is reflected back onto the electron beam, its optical path difference in a cycle, e. g. $F_1A\rightarrow AB\rightarrow BF_1$, can be expressed as:

$$\begin{aligned}\delta &= \sqrt{[y_A-(-f)]^2+x_A^2}\\ &\quad+\sqrt{[y_A-y_B]^2+(x_A-x_B)^2}\\ &\quad+\sqrt{[y_B-(-f)]^2+x_B^2}\\ &=4a \end{aligned} \quad , \quad (3)$$

where f is focal length. The results show that all radiation rays with the emission angle $\theta=\pi/2$ and random azimuthal angles, emitted by the electron beam at the focus, F_1, can be reflected back onto the electron beam with same-phase. When

$$4a=k\lambda \quad , \quad (4)$$

where k is a positive integer, all radiation rays is enhanced by the phase matching so as to produce the high peak power photon.

It can be proved that if the emission angle $\theta\neq\pi/2$, e. g. $\theta=1.3$, all radiation rays with the emission angle $?=1.3$ and random azimuthal angles, emitted by the electron beam, still can be reflected back onto the electron beam from the surface of elliptical mirror with same-phase. In this condition, Eq. (4) should be expressed as:

$$\frac{4a}{\sin\theta}=k\lambda \quad . \quad (5)$$

In this experimental device of S-P radiation, as the sheet electron beam passes over the grating on the inner wall of all-feedback resonator, and along the focal line of elliptical mirror, the electromagnetic radiation is emitted in all directions. The all-feedback resonator reflect all radiation with an emission angle and random azimuthal angles which backs onto the electron beam with same-phase and cause the electrons to be modulated. If proper conditions of synchronism are met, the electron beam will be bunched and the radiation is gained gradually[11-12]. When the interaction reaches self-exciting condition, a steady state oscillation is established at one of the resonant frequencies of the all-feedback resonator. By adjusting the length of the grating period, or adjusting the voltage of the electron beam, tunable coherent S-P radiation at Terahertz wavelengths with high output power and efficiency can be observed.

2 PIC simulation of beam-wave interaction

The output characteristics of experimental device of S-P radiation based on the all-feedback resonator were studied by a PIC simulation method. In the PIC simulations, the Maxwell's equations are solved usually by the finite-difference time-domain (FDTD) code[10-15]. With the help of the 3D PIC simulation, the characteristics of S-P radiation including the radiation energy and field distribution as well as the interaction processes of electron bunches can be obtained. In this paper, the main parameters of the metallic grating and electron beam are sum-

marized in Table 1.

Figure 3(a) shows the density of electrons in longitudinal direction when bunching has occurred at time 12.099? ns and Fig. 3(b) shows the kinetic energy of electrons in bunching state at the same time. In Fig. 3, strong bunching is apparent. Evidently, a majority of electrons are in the state of losing energy and the high-frequency field is increased in power, correspondingly. By analyzing oscillations we estimated approximately 1.93 mm for the wavelength, quite consistent with the value expected from the dispersion relation. We also note that the mean energy loss is 4 ~ 5 keV or 4% ~ 5% of the beam energy.

表 1　Parameters of the simulations

Table 1　模拟参数

parameter	Value
major half axis	13.66mm
minor half axis	3.66mm
period length of metallic grating	1.5 mm
depth of metallic grating	0.68 mm
metallic width of metallic grating	0.5 mm
number of periods	50
beam voltage	100 kV
beam current	1.3 A
transverse size of beam	0.5 mm
axial magnetic field	2.0 T

Figure 4(a) gives the contour map of the electromagnetic field components *Ex*, *Ey*, *Ez*, *Bx*, *By* and *Bz* at *y*-*z* plane at time $t = 8.977$ ns, Fig. 4(b) gives the contour map of the electromagnetic field components *Ex*, *Ey*, *Ez*, *Bx*, *By* and *Bz* at *x*-*z* plane at same time, and Fig. 4(c) gives the contour map of the electromagnetic field components *Ex*, *Ey*, *Ez*, *Bx*, *By* and *Bz* at *y*-*x* plane at same time. From Fig. 4, we can see that the distribution of field displays regular distribution and the emission angle is about $\theta \approx 0.9598$. According to Eq. 1, the corresponding frequency is about 159.838 GHz at $\theta \approx 0.9598$. It should be noted that this kind of filed distribution is beneficial to improving the efficiency of beam-wave interaction. From the size of filed distribution, we can draw a conclusion that as a sheet electron beam passes over the grating on the inner wall of all-feedback resonator, and along the focal line of elliptical mirror, a steady state high-frequency field can be established at one of the resonant frequencies of the all-feedback resonator. By calculating filed distribution, we also estimated approximately 1.93 mm for the wavelength of high-frequency field.

The evolution curve of field power S. DA and the corresponding FFT at output port are shown in Fig. 5. Apparently, there exist two different types of radiation. One is diffraction emission originated from the evanescent wave and diffracted at the ends of grating, whose frequency is the evanescent frequency (77.740 GHz). The other is the so-called SP-FEI radiation originated from ordinary SP radiation but enhanced by the micro-bunching of electron beam in some special direction corresponding to the second harmonic (or the third harmonic) of the evanescent wave[12,14]. As the beam-wave interaction reaches

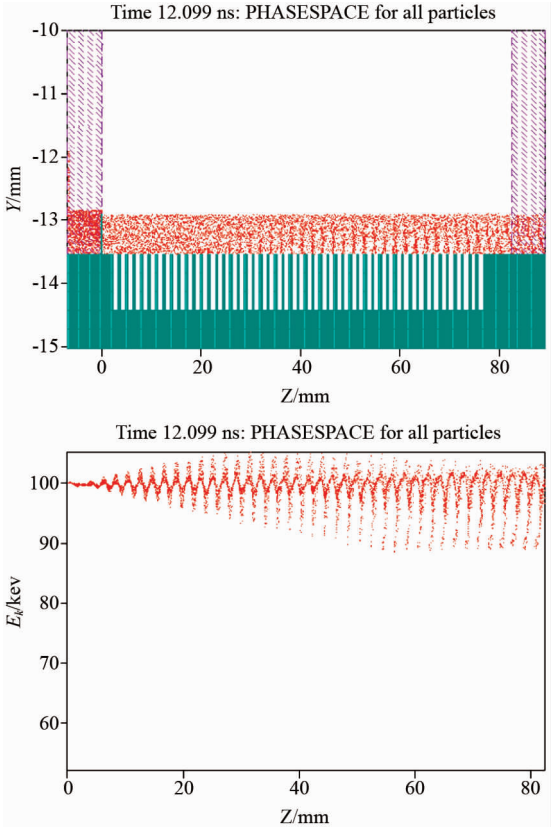

Fig. 3　Phase-space distribution. (a) density of electrons in the *z*-*y* plane at 12.099 ns, bunching is evident; (b) kinetic energy of electrons in bunching state

图 3　(a)12.099 ns 时 *z*-*y* 平面上的电子密度分布. (b) 群聚状态的电子动能

self-exciting condition, the radiation field begins to increase rapidly. In Fig. 5, the time signal shows rapid growth about 5 ns later. From the FFT amplitude, the dominant radiation is the second harmonic (155.480 GHz) or the third harmonic (233.436 GHz), which peaks at the emission angle of about $\theta \approx 1.002$ or $\theta \approx 0.254$ corresponding to the SP radiation angle predicted by Eq. 1. Of course, there is a slight discrepancy between the simulation data for the frequency of 155.480 GHz and the theoretical value 159.838 GHz of the basic SP equation at $\theta \approx 0.9598$. If we consider the mean energy loss (5 keV) and according to Eq. 1, the practical wavelength of the S-P radiation $\lambda \approx 1.93$ mm at the emission angle $\theta \approx 0.9598$ and the corresponding frequency $\nu \approx 155.480$ GHz, quite consistent with the frequency of the dominant radiation. From the contour plot of Fig. 4(a), one can easily understand that the dominant second harmonic radiates at the emission angle of about $\theta \approx 0.9598$.

3　Conclusions

It can be concluded from the simulation results that tunable coherent S-P radiation at Terahertz wavelengths can be generated by this novel grating-resonator composite structure. We also can find that this novel grating-re-

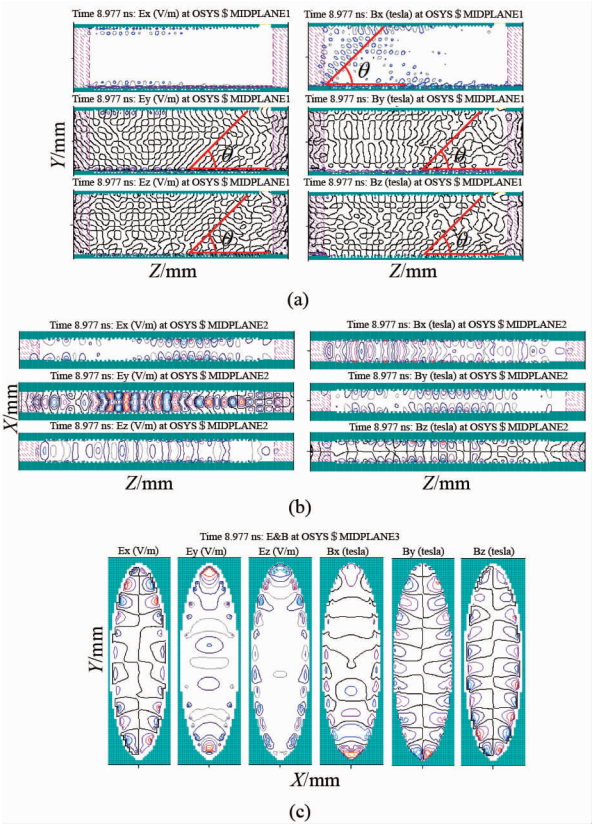

Fig. 4 Contour map of the electromagnetic field components
图 4 电磁场分量的等值线图

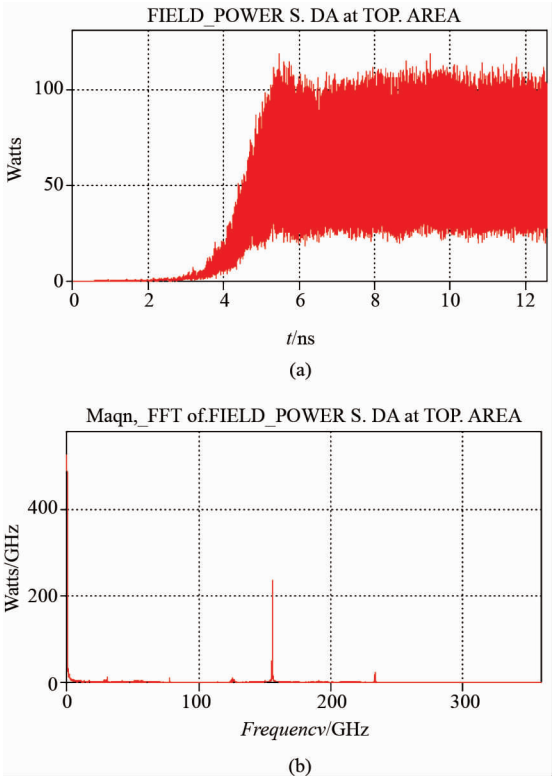

Fig. 5 The evolution curve of field power at output port. (a) the field power S. DA; (b) the corresponding FFT.
图 5 (a)输出端口的场功率曲线. (b)对应的快速傅立叶分析

sonator composite structure has the following advantages: it can reflect all radiation with an emission angle and random azimuthal angles which backs onto the electron beam with the same phase and cause the electrons to be modulated.

Acknowledgments

This work was supported by the National Natural Science Foundation of China under Grant No. 11275089 and 11375081.

References

[1] Smith S J , Purcell E M, Visible light from localized surface charges moving across a grating, *Phys Rev.* 1953,**92**:1069.
[2] Doria A , Gallerano G P , Giovenale E *et al.* , Can coherent Smith-Purcell radiation be used to determine the shape of an electron bunch, *Nucl Instrum Methods A* 2002,**483**:263 - 267.
[3] Urata J, Goldstien M, Kimmitt M F, Superradiant Smith-Purcell emissions, *Phys Rev Lett*,1998,**80**: 515 - 519.
[4] Liu C S , Tripathi V K, Stimulated coherent Smith-Purcell radiation from a metallic grating, *IEEE J Quantum Electron*, 1998,**34**:1503 - 1507.
[5] Wachtel J M, Free-electron lasers using the Smith-Purcell effect, *J Appl Phys*, 1979,**50**(1): 49 - 56.
[6] Andrews H L, Boulware C H ,Brau C A ,*et al.* , Super-radiant emission of Smith-Purcell radiation, *Phys Rev STAB* 2005,**8**:110702.
[7] Marshall T C, Free electron lasers, Macmillan Publishing Company, New York ,1985.
[8] Backe H, Lauth W , Mannweiler H, *et al.* Investigation of Far-Infrared Smith-Purcell Radiation at the 3.41Mev electron injector linac of the Mainz microtron mami. Advanced Radiation Sources and Applications (NATO Science Series II: Mathematics, Physics and Chemistry),2006,**199**:267 - 282.
[9] Meng X Z, Wang M H , Ren Z M. Analysis of high brightness laser synchrotron source based on the technique of oval supercavity, *Acta Phys Sin* 2010,**59**:1638.
[10] Meng X Z, Wang M H , Ren Z M. Smith-Purcell Free electron laser based on the semi-elliptical resonator, *Chin. Phys. B* 2011, **20**: 05072.
[11] Wang M H, Liu P K , Ge G Y, *et al.* , Free electron laser based on the Smith-Purcell radiation, *Optics & Laser Technology*,2007,**39**:1254 - 1257.
[12] Meng X Z, Smith-Purcell free electron laser based on a semi-conical resonator *Optics Communications* 2012,**285**:975 - 979.
[13] Bei H, Dai D D, Dai Z M. Simulation of Smith-Purcell radiation from compact terahertz source, *High Power Laser & Particle Beams*,2008 , 20:2067.
[14] Gao X, Yang Z Q, Qi L M, *et al.* , Three-dimensional simulation of Ka-band relativistic Cherenkov source with metal photonic-band-gap structures, *Chin. Phys. B* ,2009,**18**:2452.
[15] Meng X Z, Smith-Purcell free electron laser based on a multilayer metal-dielectric stack *Optik*, 2013,**124**:3162.